Cell, Vol. 105, 575–585, June 1, 2001, Copyright ©2001 by Cell Press

A Novel Cellular Phenotype for Familial Hypercholesterolemia due to a Defect in Polarized Targeting of LDL Receptor

Ulla-Maija Koivisto,[1] Ann L. Hubbard,[2] and Ira Mellman[1,3]
[1] Department of Cell Biology
Ludwig Institute for Cancer Research
Yale University School of Medicine
333 Cedar Street
PO Box 208002
New Haven, Connecticut 06520
[2] Department of Cell Biology
Johns Hopkins University School of Medicine
725 North Wolfe Street
Baltimore, Maryland 21205

Summary

Basolateral targeting of membrane proteins in polarized epithelial cells typically requires cytoplasmic domain sorting signals. In the familial hypercholesterolemia (FH)-Turku LDL receptor allele, a mutation of glycine 823 residue affects the signal required for basolateral targeting in MDCK cells. We show that the mutant receptor is mistargeted to the apical surface in both MDCK and hepatic epithelial cells, resulting in reduced endocytosis of LDL from the basolateral/sinusoidal surface. Consequently, virally encoded mutant receptor fails to mediate cholesterol clearance in LDL receptor-deficient mice, suggesting that a defect in polarized LDL receptor expression in hepatocytes underlies the hypercholesterolemia in patients harboring this allele. This evidence directly links the pathogenesis of a human disease to defects in basolateral targeting signals, providing a genetic confirmation of these signals in maintaining epithelial cell polarity.

Introduction

Regulation of plasma low density lipoprotein (LDL) concentrations takes place primarily in the liver, the major site of both LDL production and catabolism. The ability of the liver to maintain whole body cholesterol homeostasis is in turn greatly dependent on the activity of specific LDL receptors (LDLR) that mediate the endocytic uptake of LDL. This fact is best illustrated by the decreased hepatic clearance of plasma LDL in patients with familial hypercholesterolemia (FH), a disease caused by genetic defects in the LDLR pathway (Hobbs et al., 1992). The resultant high LDL levels lead to premature atherosclerosis and coronary heart disease. Consequently, sufficient numbers of functional LDLRs must be expressed on the plasma membrane to maintain normal cholesterol levels. Furthermore, to promote removal of LDL from plasma, the receptors must be expressed in a polarized fashion at the hepatocyte sinusoidal surface.

The basic strategies governing the ability of epithelial cells to selectively target membrane and secretory proteins to apical or basolateral plasma membrane domains are well understood (Matter and Mellman, 1994; Drubin and Nelson, 1996). In many cases, basolateral targeting involves specific cytoplasmic domain signals. In Madin-Darby canine kidney (MDCK) cells, either of two such signals can target LDLR from the Golgi complex or from endosomes to the basolateral membrane: (1) a low capacity determinant partly colinear with the receptor's signal for endocytosis and (2) a high capacity determinant unrelated to endocytosis signals (Matter et al., 1992). These signals are at sites proximal and distal to the membrane, respectively, but both depend on critical tyrosine residues. Additionally, a glycine residue adjacent to the tyrosine residue is required for optimal function of the distal signal, as is a patch of acidic residues downstream from the tyrosine (Matter et al., 1994). Interestingly, the same glycine residue important for polarized sorting in MDCK cells is replaced by aspartic acid in FH patients harboring the FH-Turku (G823D) allele, a common FH gene in the Finnish population (Koivisto et al., 1995).

Hepatocytes are distinguished from other well-studied epithelial cells in the way they establish and maintain the polarized distribution of plasma membrane components. Based on observations in rat liver and in the hepatocyte-like WIF-B cell line, endosomes appear to be the predominant sorting site for both internalized and newly synthesized proteins in hepatocytes (Mostov et al., 1992; Bartles et al., 1987; Ihrke et al., 1998). Thus, most apical and basolateral proteins are not sorted upon exit from the trans-Golgi network (TGN). They are instead transported together to the basolateral surface where they are internalized and then directed from endosomes to their final destinations. MDCK cells, in contrast, utilize a direct sorting pathway from the TGN to the apical membrane (Matter and Mellman, 1994; Keller and Simons, 1997).

Hepatocytes are further distinguished by the fact that they do not express an epithelial cell-specific subunit (μ1B) of the AP-1 clathrin adaptor complex (Ohno et al., 1999). AP-1 adaptors containing μ1B are essential for decoding basolateral targeting signals in receptors such as LDLR in the TGN of kidney epithelia (Fölsch et al., 1999). Hepatocytes may nevertheless recognize the same array of targeting signals, as proteins that are basolateral in other epithelia are generally sinusoidal in liver (Matter and Mellman, 1994). Moreover, deletion of large segments of the LDLR cytoplasmic domain that contain known basolateral targeting signals result in apical expression in the livers of transgenic mice (Yokode et al., 1992). Yet, given the differences in sorting pathways and adaptor expression, there may be important differences in the signals used by hepatocytes versus other types of epithelial cells.

We investigated the cellular phenotype associated with the FH-Turku allele to determine if a mutation in an LDLR basolateral targeting signal could manifest itself with severe hypercholesterolemia due to the missorting of otherwise functional receptors. Our data indeed demonstrate that a mutation in a critical glycine 34 residue within the receptor's cytoplasmic tail domain affects

[3] Correspondence: ira.mellman@yale.edu

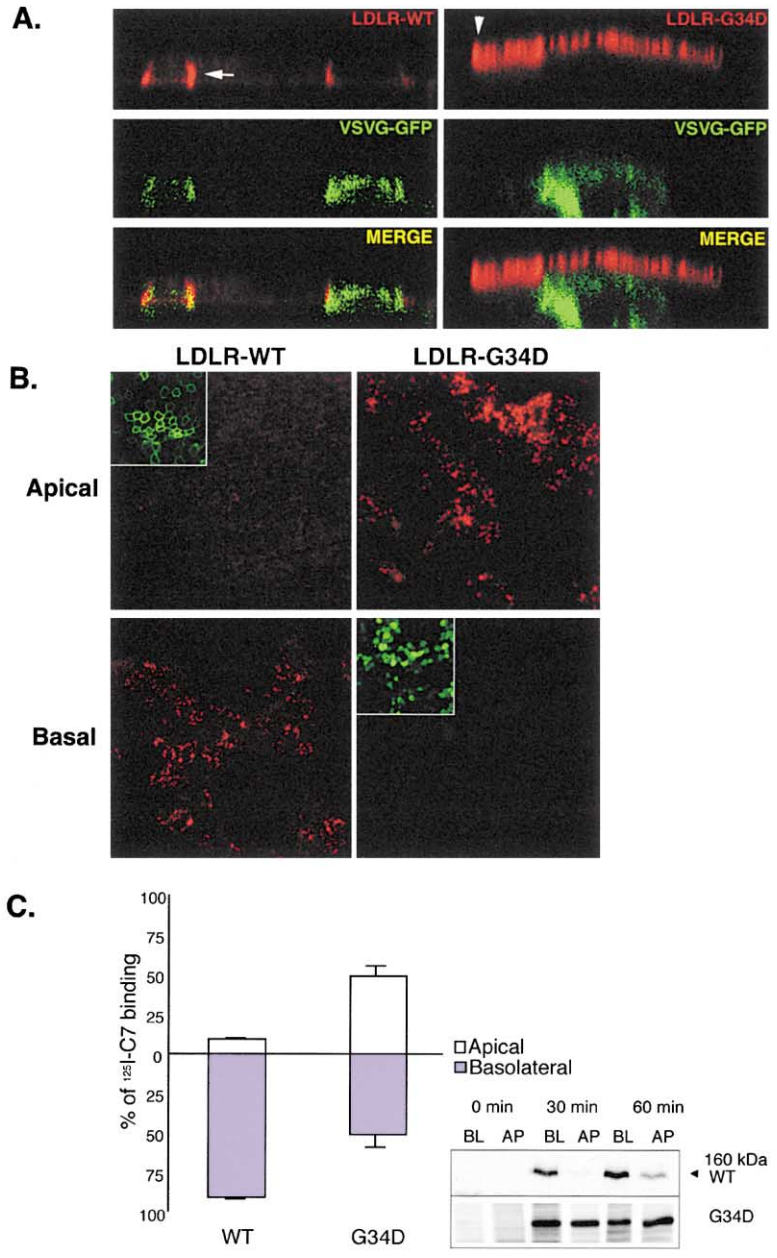

Figure 1. Functional Expression of Wild-Type and G34D Mutant LDLR in MDCK Cells

(A) LDLR-G34D is expressed on the apical surface of MDCK cells. Filter-grown MDCK cells were microinjected with expression plasmids encoding either the wild-type (left) or LDLR-G34D mutant (right) together with the VSVGts045-GFP plasmid to identify injected cells. After expression of 2 hr at 37°C and another 2 hr at 31°C, the cells were fixed and stained for cell surface LDLR expression. Vertical cross-sections (z-axis) of representative cells are shown. LDLR staining on basolateral and apical membrane domain is indicated by the arrow and the arrowhead, respectively. Green (VSVGts045-GFP), Red (LDLR).

(B) LDLR-G34D affects selectively polarized targeting without affecting endocytosis of DiI-LDL. Filter-grown MDCK cells were infected with recombinant adenoviruses encoding either the wild-type LDLR (left) or LDLR-G34D mutant (right) and analyzed for the uptake of DiI-labeled LDL. Apical endocytosis (top panels) was determined 24 hr later by continuous uptake of DiI-LDL (20 μg/ml) from the apical media for 30 min at 37°C. Endocytosis from the basolateral side (bottom panels) was determined 48 hr postinfection by binding of DiI-LDL (10 μg/ml) on the basolateral surface at 4°C for 90 min followed by 15 min incubation at 37°C. For endocytosis assays at the basolateral surface, cells were grown on filters with 3 μm pores to optimize access to LDL particles. Insets show lower magnification views of the negative panels to demonstrate the presence of expressing cells (green) that failed to internalize the ligand from the indicated plasma membrane domain.

(C) LDLR-G34D is missorted within the secretory pathway in MDCK cells. Stable cell lines expressing either the wild-type or the G34D mutant were generated and grown on permeable filter supports. LDLR polarity was analyzed by vectorial antibody binding assay in which ^{125}I-labeled C7 IgG was added either to the apical or basal media. Replacement of the glycine 34 residue by aspartic acid (G34D) resulted in a highly increased apical polarity (up to 67% apical) as compared to the wild-type receptor (up to 94% basolateral). Data shown represents means ± SE of four individual experiments each performed in triplicate.The surface distribution of newly synthesized LDLR was analyzed in the same stably transfected cell lines by domain-specific biotinylation as performed previously (Matter et al., 1992).

polarized targeting of the LDLR in both the secretory (MDCK) and endocytic (MDCK, WIF-B) pathways, and underlies the metabolic abnormality resulting in reduced liver LDL clearance in vivo.

Results

The G34D FH-Turku Mutation Affects Basolateral Targeting in MDCK Cells

The FH-Turku mutation affects a conserved glycine-tyrosine (GY) motif at positions 34 and 35 of the LDLR cytoplasmic domain (Koivisto et al., 1995). Since these residues are essential for efficient basolateral targeting in MDCK cells, we first asked if the glycine to aspartic acid mutation in FH-Turku (G34D) affected polarized sorting on its own. Previous work examined only a glycine to alanine substitution at this position in combination with a tyrosine to alanine mutation at position 18 to inactivate a second basolateral targeting signal in a membrane proximal position (Matter et al., 1994). The double mutant markedly increased apical expression (55% for the Y18AG34A double mutant as opposed to only 5%–15% for the Y18A single mutant) (Hunziker et al., 1991; Matter et al., 1994).

We expressed wild-type and FH-Turku receptors in polarized MDCK cells by cDNA microinjection or infection using recombinant adenoviruses. When injected cells were analyzed by immunofluorescence confocal

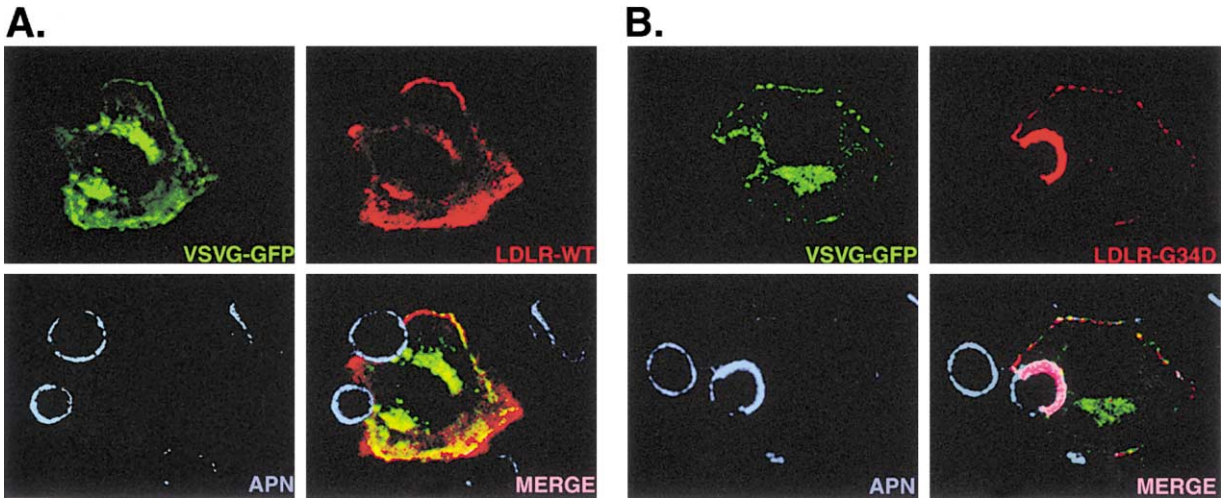

Figure 2. LDLR-G34D Is Mistargeted to the Bile Canalicular (apical) Domain in WIF-B Cells

Polarized WIF-B cells were comicroinjected with expression plasmids encoding either the wild-type LDLR (A) or LDLR-G34D mutant (B) and the VSVGts045-GFP plasmid. After >4 hr of expression at 37°C, the cells were fixed in PFA/methanol and double-stained for the localization of LDLR and the endogenously expressed APN on the bile canalicular membrane. Green (VSVGts045-GFP), Red (LDLR), Blue (APN).

microscopy, the mutant receptor (LDLR-G34D) was found mistargeted to the apical surface, while the wild-type LDLR (LDLR-WT) was expressed only on basolateral surface (Figure 1A). Identical results were obtained using the corresponding recombinant adenoviruses (not shown). Although qualitative, these results demonstrated that substitution of an aspartic acid for the glycine at position 34 effectively reversed the polarity of the LDLR.

We next confirmed that the G34D mutation had no effect on LDLR-mediated endocytosis. MDCK cells infected with a recombinant adenovirus encoding wild-type LDLR were capable of internalizing fluorescent LDL (DiI-LDL) from the basolateral but not from the apical surface (Figure 1B). Cells expressing the LDLR-G34D were also able to internalize DiI-LDL, but as expected, only from the apical side. These results were confirmed by quantitative binding and uptake assays of ^{125}I-labeled anti-LDLR antibody (C7 IgG) using transiently transfected nonpolarized CHO cells (internalization index of 1.7 for wild-type versus 1.9 for LDLR-G34D; internalization index represents internalized/bound radiolabel at 15 min [Davis et al., 1986]). Similar results were obtained in stably expressing MDCK cells grown on plastic or filters (not shown).

We also confirmed that the mislocalization of the G34D mutant reflected its missorting in the TGN. For these experiments, stable cell lines expressing the mutant or wild-type forms of the receptor were generated and then analyzed by pulse-chase radiolabeling followed by vectorial biotinylation to determine the kinetics of appearance of receptors at the apical or basolateral surfaces. As has already been well established for other LDLR targeting mutants (Matter et al., 1993, 1994), newly synthesized LDLR-G34D reached the apical surface directly from the TGN, i.e., without first having to appear at the basolateral surface; wild-type LDLR appeared directly and almost exclusively at the basolateral side (Figure 1C).

The G34D Mutation Results in Mistargeting of LDLR to the Apical Surface in Hepatic WIF-B Cells

Given the differences in sorting pathways between kidney epithelia and hepatocytes, it cannot be assumed that a mutation affecting polarity in MDCK cells will exhibit the same phenotype in hepatocytes. Thus, to determine if glycine 34 was required for basolateral targeting in hepatocytes, we analyzed the localization of the LDLR in polarized hepatic WIF-B cells (Ihrke et al., 1993).

WIF-B cells were microinjected with an LDLR expression plasmid and analyzed by confocal immunofluorescence microscopy; as before, VSVGts045-GFP was coinjected to mark expressing cells. WIF-B cells expressing wild-type LDLR exhibited a strikingly polarized pattern in which the receptor was limited to the basolateral surface of the cells (Figure 2A). The receptor was excluded entirely from the bile canalicular domain that forms between adjacent cells, illustrated by its nonoverlapping distribution with the endogenous apical marker aminopeptidase N (APN). In contrast, the G34D mutant was found predominantly at the bile canalicular domain where it colocalized with APN (Figure 2B). Relatively little staining was found at the basolateral surface. The small amount of basolateral LDLR would be consistent, however, with the predicted transient residence of newly synthesized apical proteins at the basolateral domain in hepatocytes.

Indeed, we next demonstrated directly that the G34D mutant was transcytosed across the WIF-B cells from basolateral to the apical surface. For these experiments, WIF-B cells were infected with recombinant adenoviruses encoding either the wild-type or the G34D mutant receptor, and the cells allowed to bind the anti-LDLR antibody C7 at 4°C. The cells were then washed and warmed to 37°C, and the fate of the antibody-labeled receptors monitored by immunofluorescence. Although cells expressing both wild-type and mutant receptors initially

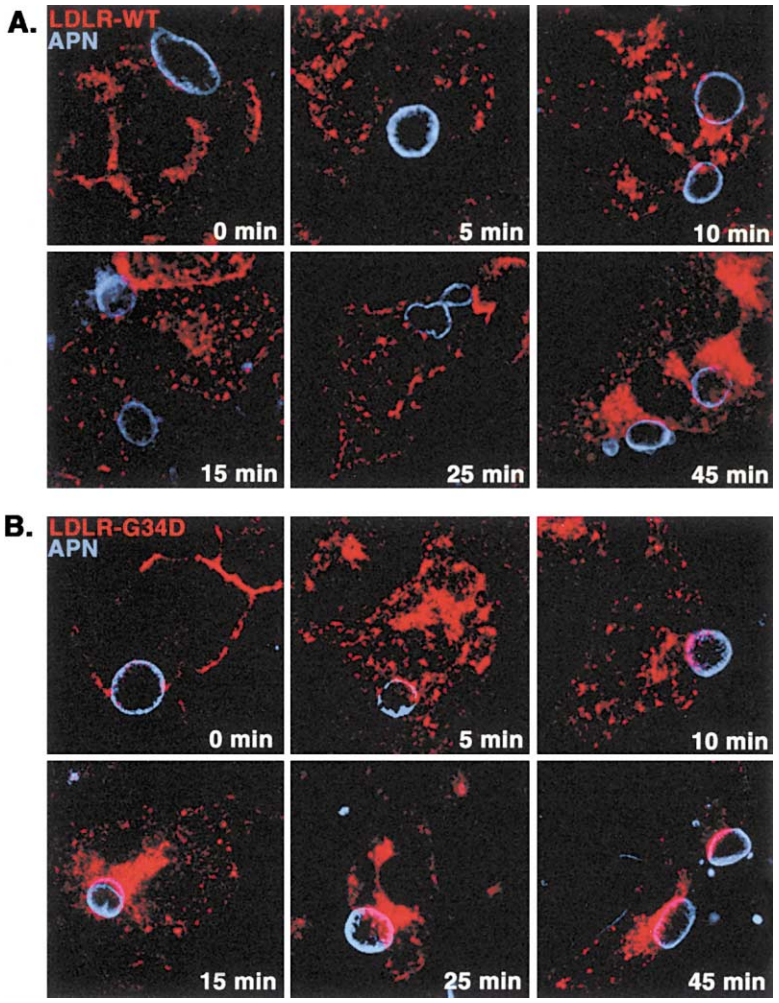

Figure 3. LDLR-G34D Reaches the Apical Domain by Transcytosis

WIF-B cells were infected with adenoviruses encoding the wild-type LDLR (A) or LDLR-G34D (B). After 24 hr of expression, the cells were placed on ice and allowed to bind C7 IgG for 30 min before washing and culture at 37°C in antibody-free medium. At the indicated times, the cells were fixed with PFA/methanol and stained for the distribution of C7 IgG-labeled LDLR and endogenously expressed canalicular marker APN. In infected cells, C7 IgG bound to LDLR-G34D, but not wild-type LDLR, began to appear at the apical surface after just 10–15 min of uptake. C7 IgG did not bind to uninfected cells. Red (LDLR), Blue (APN).

exhibited only basolateral labeling (0 min), cells expressing the G34D mutant began to show apical staining after just 10–15 min of endocytosis (Figure 3). In contrast, labeling of the antibody bound to wild-type receptors was restricted either to the basolateral plasma membrane or to intracellular vesicles and never reached the APN-positive apical domain. At longer chase times (45 min), the remaining labeled vesicles in the wild-type-expressing cells were concentrated in the apical cytoplasm just below the bile canaliculus, a location reminiscent of apical recycling vesicles in MDCK and Caco-2 cells (Apodaca et al., 1994; Knight et al., 1995; Sheff et al., 1999; Tuma et al., 1999). We suspect that C7 bound to wild-type LDLR traced the normal basolateral recycling pathway of the receptor. In any event, these results demonstrated that the G34D mutation caused apical expression largely due to missorting during endocytosis.

We next asked if the differential localization of the wild-type and mutant LDLRs in polarized WIF-B cells affected the ability of each receptor to mediate LDL uptake. Although WIF-B cells expressing wild-type LDLR (following infection with a recombinant adenovirus) exhibited significant internalization of DiI-LDL, cells expressing the LDLR-G34D accumulated very little of the fluorescent ligand (Figure 4). This presumably reflects the fact that the mutant receptors, although capable of LDL endocytosis (e.g., Figure 1B), were localized largely to the apical domain, which was sequestered by junctional complexes from the growth medium. Apparently, the relatively small amount of mutant receptor in transient residence at the basolateral surface was not sufficient to achieve significant amounts of DiI-LDL uptake.

Hepatocytes Rely Predominantly on the LDLR Distal Basolateral Targeting Signal

The LDLR cytoplasmic domain contains two distinct basolateral targeting signals, the first in a membrane proximal position and dependent on tyrosine 18, the second in a more distal COOH-terminal position and dependent on glycine 34 and tyrosine 35. In MDCK cells, the distal signal is dominant in that the elimination of tyrosine 18 by itself has little effect on basolateral polarity at moderate expression levels in stably transfected cells (Matter et al., 1992). Since this tyrosine residue is critical for LDLR endocytosis (Davis et al., 1986, 1987), we next examined its role in determining LDLR polarity in hepatocytes given the central role of endocytosis and

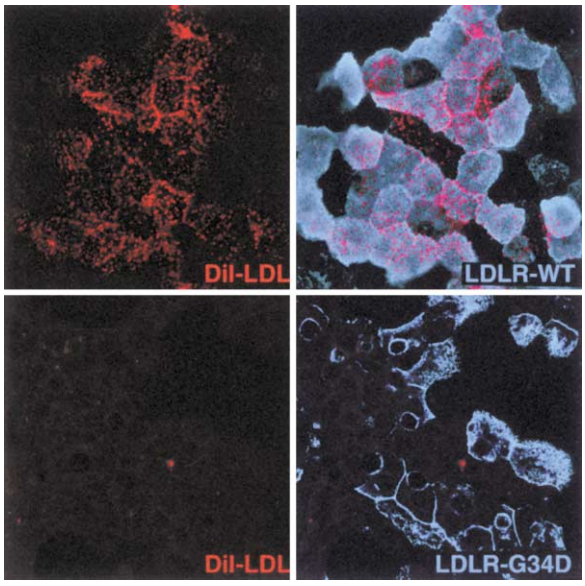

Figure 4. Polarized Distribution of the LDLR Parallels the Endocytosis of DiI-LDL from the Basolateral Surface in WIF-B Cells

WIF-B cells were infected with recombinant adenoviruses encoding either the wild-type LDLR (top) or the LDLR-G34D mutant (bottom). After 24 hr of infection, the cells were assayed for the uptake of DiI-LDL (2 μg/ml) in the growth medium by a 30 min incubation at 37°C. The cells were washed with PBS, fixed with PFA/methanol, and stained for LDLR expression. Red (DiI-LDL), Blue (LDLR).

endosomal recycling in sorting apical from basolateral membrane proteins.

We first investigated the effect of a tyrosine 18 (Y18A) mutation on LDLR polarity in microinjected or adenovirus-infected WIF-B cells. As expected, these endocytosis-defective receptors, which possessed only the distal basolateral targeting signal, were expressed predominantly at the basolateral surface (Figure 5A). Some labeling was also seen in intracellular vesicles, presumably reflecting the slow basal rate of internalization that occurs even in the absence of a coated pit signal. We next determined the distribution of LDLR double mutant in which the tyrosine 18 mutation was combined with a mutation in glycine 34 (Y18AG34D), a receptor which was not only endocytosis defective, but also devoid of all basolateral targeting information. As shown in Figure 5B, the LDLR-Y18AG34D was expressed at the apical surface to an extent similar to that seen for the G34D mutant alone (compare with Figure 2B). Given the absence of a functional coated pit signal, we next asked if the LDLR-Y18AG34D double mutant nevertheless reached the apical surface by the indirect route, following transcytosis from the basolateral surface. Indeed, by monitoring the fate of the C7 anti-LDLR antibody bound at the basolateral surface of these cells, LDLR-Y18AG34D mediated C7 IgG transcytosis, albeit more slowly than the C34D single mutant (~45 min versus 10-15 min) (Figure 6B versus Figure 3B). A mutant receptor lacking only the coated pit localization domain but retaining the distal basolateral targeting signal failed to mediate basolateral to apical transcytosis of C7 IgG (Figure 6A).

Thus, hepatocytes appear to rely predominantly, if not exclusively, on the distal glycine 34-containing basolateral targeting signal. Accordingly, we found that the effect of G34D mutation was dominant with respect to the equilibrium distribution of the receptor.

Mistargeting of the LDLR in Liver Causes Defective LDL Clearance and Underlies the Metabolic Abnormality in FH

To demonstrate directly that a defect in polarized targeting of the LDLR produces a clinical picture of severe hypercholesterolemia, we extended our cell culture observations by overexpressing the same LDLR recombinant adenoviruses in vivo using LDLR$^{-/-}$/APOBEC-1$^{-/-}$

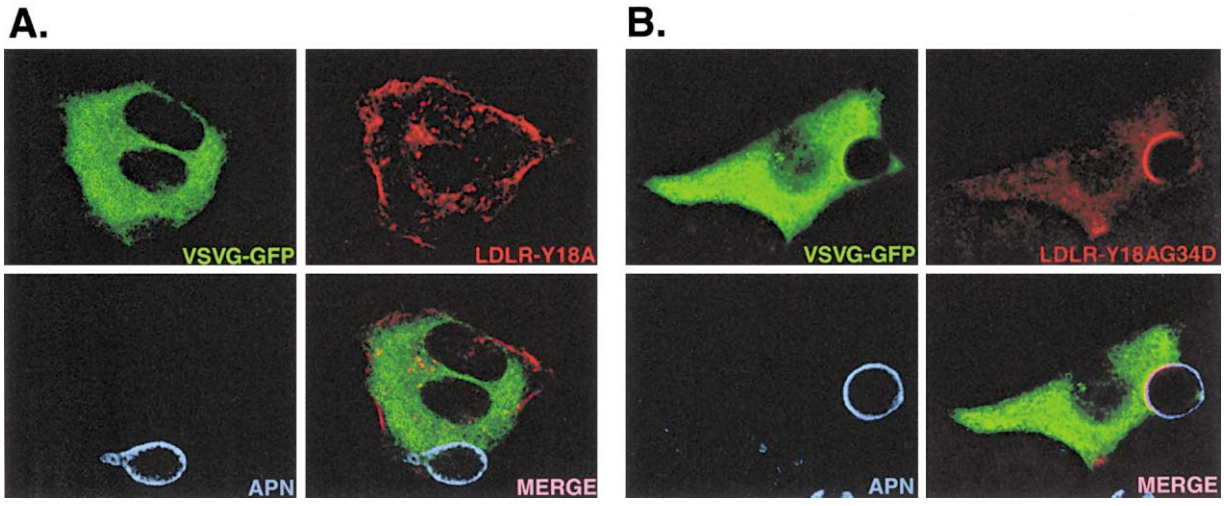

Figure 5. G34-Containing Basolateral Targeting Signal Is Dominant over the Clathrin-Mediated Endocytosis Signal

Polarized WIF-B cells were microinjected with expression plasmids encoding the endocytosis-defective mutants LDLR-Y18A (A) or LDLR-Y18AG34D (B) together with the VSVGts045-GFP plasmid. The LDLR expression was analyzed as described in Figure 2. Green (VSVGts045-GFP), Red (LDLR), Blue (APN).

mice, a mouse model of human FH (Powell-Braxton et al., 1998). Four different viruses were used, encoding LDLR wild-type, as well as G34D, Y18A, and Y18AG34D mutants.

We injected 5×10^9 pfu of each of the adenovirus-encoded transgenes intravenously into LDLR$^{-/-}$/APOBEC-1$^{-/-}$ mice. This dose resulted in a uniform expression of virally encoded receptors in a large majority of hepatocytes 4–10 days postinjection, as demonstrated by immunofluoresence microscopy of frozen liver sections stained for the human LDLR (blue) and endogenous APN (red) (Figure 7A).

To assess the polarity of LDLR expression, higher magnification images were analyzed. As previously reported (Herz and Gerard, 1993; Ishibashi et al., 1993), adenovirus-encoded wild-type human LDLR was expressed on the sinusoidal surface of hepatocytes, together with some staining on the lateral surfaces (Figure 7B, upper panels [*a*]). Importantly, the receptor was not detected at the bile canalicular membrane, visualized by staining for APN or a second apical marker dipeptidyl peptidase IV (DPPIV; arrowheads). Some DPPIV staining was also present sinusoidally, reflecting its expression by sinusoidal lining cells (arrows; see legend). The distribution of the endocytosis-defective form of the LDL (Y18A) resembled that of the wild-type LDLR (not shown).

The staining pattern of the LDLR-G34D mutant transgene was different from that of the wild-type receptor. Human LDLR was now distinctly visible at bile canalicular surface as indicated by its colocalization with DPPIV (arrowheads in Figure 7B, lower panels [b]). Similar results were obtained using three different antibodies to LDLR (see Experimental Procedures) and also using livers expressing the LDLR-Y18AG34D double mutant (not shown). Some mutant LDLR staining at sinusoidal surfaces was also observed, but these receptors were unable to mediate physiologically significant amounts of LDL uptake (see below). Therefore, the sinusoidal staining may represent LDLR expression in cells lining the sinusoids, such as endothelial, Kupfer, or other perisinusoidal cells which are susceptible to infection by recombinant adenoviruses (Yu et al., 2000).

The fact that the FH-Turku LDLR G34D was expressed largely at the apical surface suggested that it might not be accessible to plasma LDL and thus might be unable to mediate efficient clearance of plasma cholesterol. We therefore assessed the ability of wild-type versus mutant LDLR to lower the steady-state cholesterol levels in LDLR$^{-/-}$/APOBEC-1$^{-/-}$ mice. It has been previously shown that adenovirus-mediated gene transfer of the wild-type LDLR results in an acute reversal of hypercholesterolemia in LDLR knockout mice (Ishibashi et al., 1993) and also accelerates cholesterol clearance in normal mice (Herz and Gerard, 1993). We similarly found that the plasma steady-state total cholesterol levels in the LDLR$^{-/-}$/APOBEC-1$^{-/-}$ mice intravenously injected with 5×10^9 pfu of the wild-type LDLR recombinant virus decreased drastically upon overexpression of the virally encoded LDLR. Four days after virus infection, the total plasma cholesterol in a cohort of six mice was reduced by up to 88% (average decrease of 78 $\pm$ 3 SEM%), and the effect of the transgene expression on reducing cholesterol levels persisted in individual mice for at least 10 days (Figure 8A).

In contrast, adenovirus-mediated expression of the G34D mutant had little effect on steady-state cholesterol levels (Figure 8A). Although a small decrease was observed at day 4 in a few mice, this possibly reflected high viral overexpression in general that might have resulted in some uptake by extrahepatic or nonparenchymal liver cells (e.g., Kupfer cells, see above). More impor-

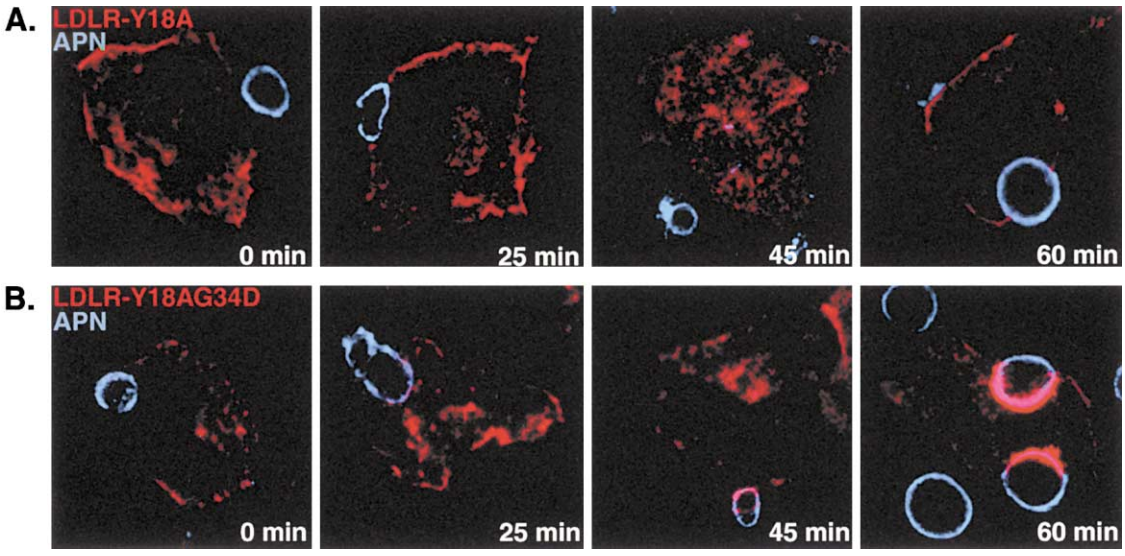

Figure 6. Apical Localization of the LDLR-Y18AG34D Requires Basolateral Endocytosis

WIF-B cells expressing virally encoded endocytosis-defective mutants LDLR-Y18A (A) or LDLR-Y18AG34D (B) were assayed for basolateral-to-apical transcytosis of the C7 IgG-labeled LDLR as described in Figure 3. While the absence of a functional clathrin-coated pit localization signal alone (LDLR-Y18A) had no effect on LDLR polarity, the cells expressing LDLR-Y18AG34D began to exhibit apical staining after ~45 min of endocytosis. Red (LDLR), Blue (APN).

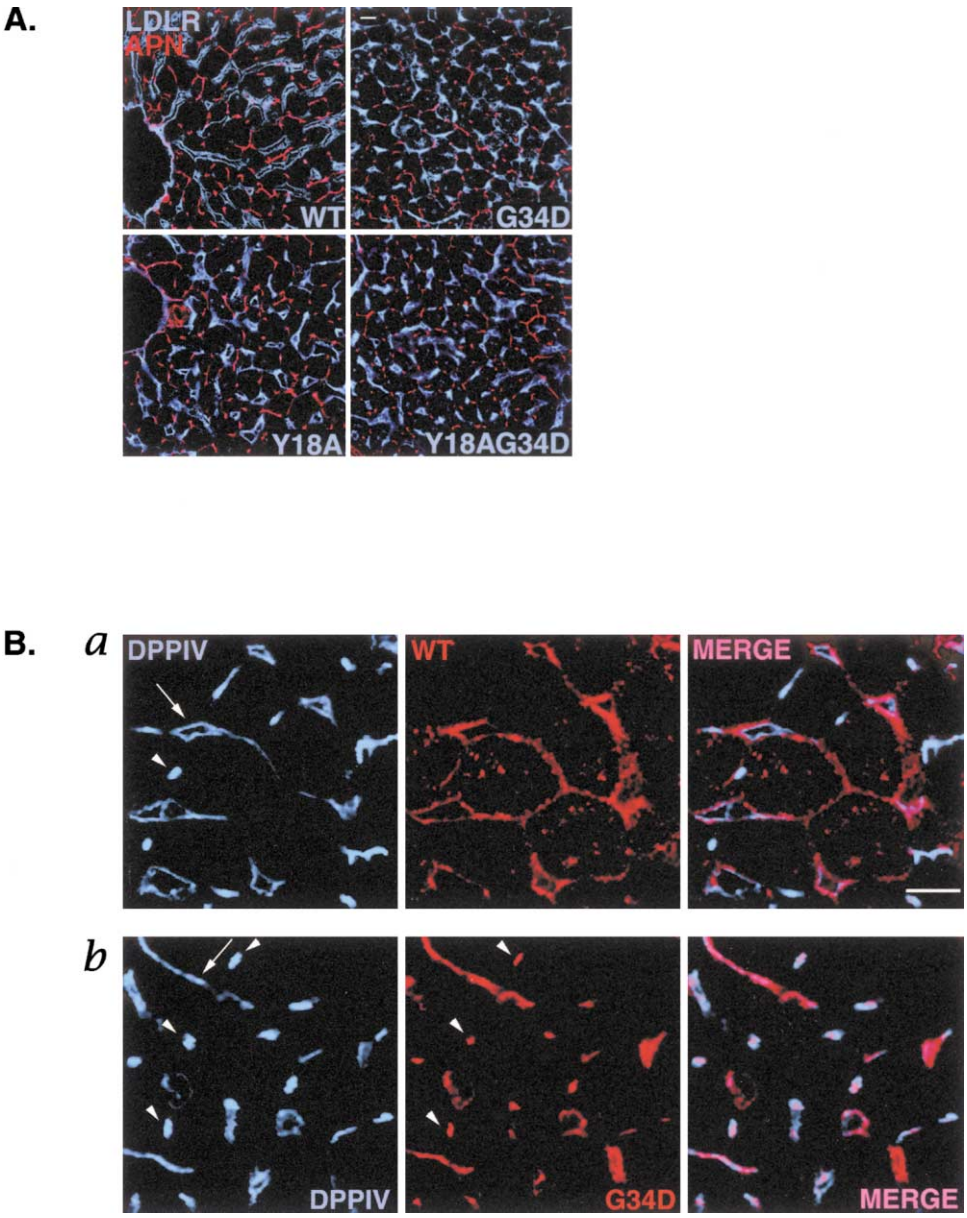

Figure 7. Expression of the Virally Encoded Wild-Type and Mutant LDLRs in Mouse Liver In Vivo

LDLR$^{-/-}$/APOBEC-1$^{-/-}$ mice were injected with 5×10^9 pfu of the indicated adenovirally encoded LDLR and perfused 4–5 days postinjection. Expression of LDLR was analyzed in frozen liver sections by indirect immunofluoresence. Low power survey view (A) of mouse liver sections stained with a monoclonal C7 IgG to LDLR (blue) demonstrated comparably efficient expression of the virally encoded wild-type and mutant LDLRs in the majority of hepatocytes. Bile canaliculi were stained for the endogenously expressed apical protein APN (red). High power view (B) of liver sections from mice expressing either the virally encoded wild-type LDLR (*a*/top) or the LDLR-G34D (*b*/bottom), stained using a rabbit polyclonal antibody to bovine LDLR (Yokode et al., 1992) (red). Bile canaliculi (arrowheads) were stained with a monoclonal antibody against DPPIV (blue) that also stains the hepatic endothelium lining the sinusoids (arrows). The wild-type LDLR was expressed exclusively on the sinusoidal surface of hepatocytes while the G34D mutant was also detectable from the bile canalicular surface. Scale bar represents 10 μm. (a: wild-type LDLR; b: LDLR-G34D; red [LDLR], blue [DPPIV]).

tantly, when the entire cohort of 17 mice was analyzed with all time points combined, total plasma cholesterol levels remained similar to preinjection levels (average 91 ± 8 SEM% of preinjection levels). Moreover, when cholesterol levels were directly compared in age- and sex-matched littermates used within this series of experiments, only the adenovirus encoding the wild-type LDLR was able to reverse the hypercholesterolemia at any time point. Similar results were obtained in mice infected with LDLR mutants affecting the coated pit localization signal alone (Y18A) or in combination with the glycine 34 mutation (Y18AG34D). Both endocytosis-defective receptors were unable to reduce starting cholesterol levels. At days 4–10, cholesterol levels in mice expressing the Y18A mutant remained at 98% of preinjection levels (±14 SEM%, n = 5 mice); at days 4–7,

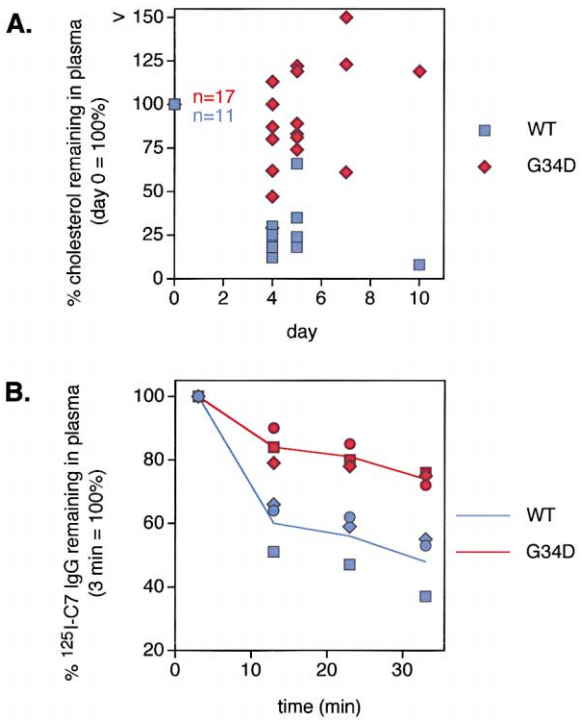

Figure 8. LDLR-G34D Does Not Correct the Metabolic Abnormality in LDLR$^{-/-}$/APOBEC-1$^{-/-}$ Mice

(A) Expression of mutant LDLR fails to correct hypercholesterolemia in LDLR$^{-/-}$/APOBEC-1$^{-/-}$ mice. Steady-state total plasma cholesterol levels (mg/dl) were measured before and at the indicated day after the injection of 5×10^9 pfu of either the adenovirally encoded wild-type LDLR or the LDLR-G34D mutant. The total cholesterol remaining in the plasma was plotted as a percentage of total cholesterol prior to injection. Squares (blue) denote the mice injected with the adenovirus encoding the wild-type LDLR, diamonds (red) denote the mice injected with the adenovirus encoding the LDLR-G34D.

(B) LDLR-G34D fails to mediate rapid clearance of intravenously injected ^{125}I-C7 IgG from plasma. Six mice expressing either the wild-type (blue) or LDLR-G34D mutant (red) were studied in sex-matched littermate pairs (identical symbols) for the plasma clearance of ^{125}I-labeled (7.5×10^6 cpm) anti-LDLR antibody C7 IgG (Huettinger et al., 1984). Four days postinjection, the mice were anesthetized, ^{125}I-C7 IgG was injected into the retro-orbital sinus, and blood was collected from the contralateral sinus at the indicated intervals. The trichloroacetic acid-precipitable radioactivity remaining in plasma was plotted as a percentage of the radioactivity in a plasma sample obtained shortly (3 min) after injection. For each average curve, two LDLR$^{-/-}$/APOBEC-1$^{-/-}$ mice (circles, diamonds) and one wild-type mouse (squares) were studied.

the Y18AG34D mice remained at 93% of control (±10 SEM%, n = 4 mice).

To directly evaluate the effect of G34D mutation on cholesterol clearance, we next analyzed the clearance rate of intravenously administered ^{125}I-labeled C7 IgG in mice overexpressing either the wild-type LDLR or the G34D mutant. The clearance rate of intravenously administered ^{125}I-labeled C7 IgG was rapid in mice expressing the wild-type transgene, with 40% of injected dose removed from plasma between 3 and 10 min after the radioactive bolus (Figure 8B). Consistent with the lack of effect on steady-state cholesterol levels, the rate of disappearance of intravenously administered ^{125}I-C7 IgG was delayed markedly in mice expressing the LDLR-G34D transgene. Thus, functional LDLR expression at the sinusoidal surface was disrupted by the G34D mutation.

Taken together, our results on the localization and function of LDLR both in cell culture and in vivo provide direct evidence that a mutation affecting the glycine 34 residue produces a receptor that cannot promote the proper plasma LDL clearance by the liver due to its altered polarity of expression in hepatocytes. Consequently, mistargeting of the LDLR is likely to account for hypercholesterolemia in patients harboring the FH-Turku allele.

Discussion

Systematic analysis of LDLR phenotypes associated with various FH alleles has revealed a range of mutations that directly or indirectly reduce the ability of the receptor to mediate endocytosis of plasma lipoproteins containing apo B-100 and/or apo E. To date, mutations have been described that diminish ligand binding, block the synthesis or surface delivery of LDLR, or prevent the internalization or recycling of otherwise functional receptors (Hobbs et al., 1992). Study of mutant LDLRs has been critical to developing current concepts in cell biology, particularly in the case of receptor-mediated endocytosis (Davis et al., 1986). Our work has added an additional element by showing that the FH phenotype can also result from a defect in polarized targeting in epithelial cells. By affecting an amino acid residue essential for proper basolateral transport, the FH-Turku allele has emphasized the functional importance of LDLR expression at the sinusoidal surface of hepatocytes. Moreover, the fact that the same conserved residue is required for basolateral expression in both hepatocytes and MDCK cells strongly suggests that both cell types make use of common targeting signals; this despite their use of different pathways for polarized protein sorting and transport.

We used several independent experimental approaches to show that the G34D mutation is responsible for mistargeting the LDLR from the basolateral to the apical membrane domain in hepatocytes. Consequently, the mutant receptor fails to mediate a physiologically relevant increase in LDLR activity on the sinusoidal membrane, resulting in retarded LDL clearance in vivo. Although we have not excluded the possibility that some mutant LDLR can follow the direct pathway to the apical surface, we found that the predominant expression of the G34D mutant on the apical surface was largely due to basolateral to apical endocytosis. Thus, the mutant receptor appears to be transported from the TGN to the sinusoidal plasma membrane along with other basolateral proteins. After internalization, the absence of a functional basolateral targeting signal would render less efficient the recycling of the G34D mutant back to the sinusoidal domain; instead, it would be transcytosed to the apical surface in a fashion analogous to the well-characterized polymeric immunoglobulin receptor (Mostov, 1994). Although a direct pathway to the apical surface has recently been reported in hepatocytes, it seems thus far to be used only by certain polytopic canalicular membrane proteins (e.g., ABC transporters) (Kipp and Arias, 2000).

The question of polarized transport in hepatocytes has re-emerged as an important issue since hepatocytes do not express the epithelial cell-specific clathrin AP-1 adaptor subunit μ1B (Ohno et al., 1999). In other epithelia, μ1B-containing AP-1B complexes have been shown to be required for basolateral transport of proteins such as LDLR by directly interacting with the receptor's basolateral targeting signals (Fölsch et al., 2001). In liver, due to a predominant reliance on indirect endosomal sorting, it is possible that AP-1A or AP-2 complexes substitute functionally for AP-1B. Conceivably, AP-1A may function in association with a nonadaptor component that modifies its activity in a fashion analogous to the action of PACS-1 or TIP47 in the transport of proteins between the TGN and endosomes (Diaz and Pfeffer, 1998; Wan et al., 1998). Alternatively, hepatocytes make use of another yet to be described adaptor-sorting system. AP-3 complexes are associated with lysosomal transport and thus do not seem likely to fulfill this role; the ubiquitously expressed AP-4 complex is without a clear functional assignment, but is expressed at low levels making its involvement in a quantitatively important transport event unlikely (Bonifacino and Dell' Angelica, 1999).

Our functional data demonstrate that expression of the G34D mutant LDLR does not replace wild-type LDLR function in transgenic mice. Thus, the decreased LDL clearance in FH patients harboring the FH-Turku allele most likely reflects a defect in LDLR polarity. Adenovirus-mediated expression resulted in the appearance of mutant, but not wild-type, receptor at the bile canalicular membrane. Nevertheless, a significant amount of mutant LDLR, like the wild-type, was also present at the sinusoidal surface. The reasons for this were not entirely clear, although it is likely that some of the receptor becomes expressed by sinusoidal endothelial cells which are also susceptible to adenovirus infection (Yu et al., 2000). Expression of the receptor in these nonparenchymal cells would not be expected to influence plasma cholesterol levels appreciably.

On the other hand, overexpression of LDLR might cause an increase in the absolute amount of the apically targeted receptor mutant in transient residence at the hepatocyte sinusoidal domain. The amount of sinusoidal LDLR-G34D is apparently insufficient, however, to mediate the endocytosis of enough plasma LDL to affect whole body cholesterol levels. The situation may be further exacerbated by saturation of the endocytosis or sorting machinery present at the sinusoidal surface (Matter et al., 1993; Marmorstein et al., 2000). A similar situation was observed upon expression of the G34D mutant in WIF-B cells. Despite the presence of at least some receptor at the basolateral surface, little uptake of DiI-LDL was observed. In a previous study (Yokode et al., 1992), a mutant LDLR containing only the first 22 amino acids of the cytoplasmic tail and thus lacking all basolateral targeting information was found primarily at the bile canalicular membrane in transgenic mice. Thus, under conditions of transgenesis likely to yield far lower expression levels, and also under conditions when expression was driven by a liver-specific promoter, a greater fraction of an apically targeted LDLR appeared uniquely at the bile front.

In any event, the fact that individuals harboring the FH-Turku allele manifest with severe hypercholesterolemia provides the most reliable and by far the most physiologically relevant demonstration of the importance of GY-based targeting signals in the maintenance of LDLR polarity. While there are other clinical disorders which are associated with alterations in polarity, these do so by affecting mechanisms which are quite different from and less well understood than that described here. For example, overall defects in vesicular targeting may underlie disorders such as autosomal dominant polycystic kidney disease (Charron et al., 2000) and microvillus inclusion disease affecting intestinal epithelia (Ameen, 2000); the mechanisms responsible for these phenotypes are unknown. Another example is a cystic fibrosis allele exhibiting a large deletion that removes a segment of the CFTR cytoplasmic tail containing a PDZ domain-interacting motif (Moyer et al., 1999). Normally apical, the mutant protein becomes nonpolarized in MDCK cells, but neither the mechanism of this effect nor its pathological consequences are understood.

In summary, we have functionally characterized the FH-Turku allele of the LDLR and shown that a substitution of a glycine 34 residue results in a defect in polarized targeting of the receptor in hepatocytes. This feature is entirely sufficient to generate an FH phenotype. Thus, the mutation affects the signals that specify basolateral targeting within polarized epithelial cells and, as such, provides a genetic proof that work on basolateral targeting using in vitro systems has revealed a physiologically important aspect of epithelial cell polarity.

Experimental Procedures

Plasmids

All transfection constructs were generated and expressed in the CMV-based eukaryotic expression vector pCB. The cDNA encoding a wild-type LDLR with an additional HindIII site in the membrane-spanning domain has been described previously (Hunziker et al., 1991). The C-terminal mutants of LDLR were constructed by replacing the HindIII/XhoI fragment of the wild-type LDLR plasmid with fragments generated by PCR using appropriate mutagenic primers. The sequences of all primers are available on request. For microinjection experiments, cDNAs encoding wild-type and mutant LDLR were subcloned in a CMV-based expression vector pRK5. The sequences of all cloned fragments were verified by automated DNA sequencing. The VSVGts045-GFP in pRK5 has been described elsewhere (Kroschewski et al., 1999).

Recombinant Adenoviruses

Recombinant adenoviruses encoding C-terminal variants of LDLR were generated according to the method described by He et al. (He et al., 1998). The adenovirus encoding the wild-type LDLR was obtained from James Wilson (University of Pennsylvania). The virus particles for intravenous injections were further purified by CsCl density gradient followed by dialysis against 10% glycerol in PBS and finally sterilized through 0.22 μm filter.

Cell Culture

MDCK (strain II) cells were cultured in DMEM with 10% fetal bovine serum (FBS) and plated for experiments onto permeable Transwell polycarbonate filters (Corning Costar) at a density of 1×10^5 cells/cm^2. Stable cell lines were obtained by the calcium phosphate precipitation method followed by clonal selection with G418 (500 μg/ml). WIF-B cells were grown in 7% CO_2 in modified Ham's F12 medium with HAT (10 mM hypoxanthine, 0.04 mM aminopterin, 1.6 mM thymidine) containing 5% FBS and plated for experiments on glass coverslips at a density of 1.3×10^4 cells/cm^2. Experiments

were performed on cells that had reached their maximal density and polarity (WIF-B 10–12 days, MDCK 4 days).

Antibodies

The following primary antibodies were used: C7 IgG, a mouse monoclonal antibody to the LDLR extracellular domain (obtained from ATCC) (Beisiegel et al., 1981), the 4A4 monoclonal antibody to the LDLR cytoplasmic domain (obtained from ATCC) (van Driel et al., 1987), a rabbit anti-bovine LDLR antiserum (the generous gift of Richard G.W. Anderson, Dallas), a rabbit anti-APN antiserum (Ihrke et al., 1993), and a guinea pig anti-DPPIV antiserum (Ihrke et al., 1993). Affinity-purified, fluorescently labeled secondary antibodies were obtained from Molecular Probes or Jackson ImmunoResearch.

Microinjection and Immunofluorescence Microscopy

MDCK and WIF-B cells were comicroinjected with the indicated LDLR (0.24 μg/μl) and VSVGts045-GFP plasmids (0.1 μg/μl) using an Eppendorf Transjector 5246 microinjection system mounted on a Zeiss Axiovert S100TV inverted microscope. After variable expression times, WIF-B cells were fixed with 4% PFA diluted in PBS, permeabilized in methanol at 4°C, and stained in PBS solution containing 1% BSA. MDCK cells were fixed with 4% PFA diluted in PBS and stained in PBS solution containing 10% goat serum. Injected cells were identified by green fluorescent protein (GFP) fluorescence. Confocal immunofluorescence microscopy was performed with a Zeiss LSM 510 laser scanning microscope. Images were processed using Adobe® Photoshop® (Adobe Systems, Inc.) version 5.5 software.

Animal Procedures

Homozygous breeding pairs of the LDLR$^{-/-}$/APOBEC-1$^{-/-}$ -mice were obtained from Genentech, Inc (South San Francisco, CA). All experiments were performed on sex-matched littermates (20–30 g) generated following 2–3 crosses of the original breeding pairs and fed ad libitum a regular chow diet throughout the study. Each recombinant adenovirus was injected as a single dose (5×10^9 pfu) either via the tail vein or into the retro-orbital sinus of an anesthetized mouse. Blood samples (50–100 μl) were collected by retro-orbital bleeding from the nonfasted anesthetized animals. Animal experiments were approved by the Yale Animal Care and Use Committee (YACUC) and were performed according to all applicable federal animal welfare policies and regulations.

Immunohistochemistry

Mice were anesthetized by intraperitoneal ketamine (100 mg/kg) and transcardially perfused with PBS followed by ice-cold 2% PFA in PBS. Livers were then removed and postfixed in the same fixative for 1–2 hr, followed by cryoprotection in 0.5 M sucrose solution at 4°C. Pieces of liver were embedded in TBS medium (Triangle Biomedical Sciences) and quick-frozen in isopentane. Indirect immunofluorescence was performed on 7 μm-thick cryosections that were fixed in methanol at −20°C, rehydrated in PBS, and stained overnight with the indicated antibodies in PBS containing 1.5% BSA, 0.3% Triton X-100.

Biochemical Assays

Binding and internalization of ^{125}I-labeled anti-LDLR antibody C7, cell surface biotinylation, and immunoprecipitation were performed as described (Matter et al., 1992). Uptake of DiI-LDL (Molecular Probes) was visualized after incubation of the cells at 37°C with the indicated ligand concentration in the medium followed by three washes with PBS. The transcytosis assay was performed essentially as described (Ihrke et al., 1998). Plasma cholesterol levels were determined enzymatically using Sigma Diagnostics (St. Louis) cholesterol reagent. Plasma content of ^{125}I-labeled (specific activity 1.5×10^6 cpm/μg) C7 IgG was measured by trichloroacetic acid precipitation followed by γ counting. Data are shown as mean ± SEM.

Acknowledgments

We thank L. Powell-Braxton for the LDLR$^{-/-}$/APOBEC-1$^{-/-}$ mice; L. Breiterman and M. Bastaki for providing the WIF-B cell line and antibodies; C. Soroka for advice on liver histology; and all helpful colleagues of the Mellman/Warren laboratory.

This work was supported by a grant from the NIH (GM29765) to I.M., who is also a member of the Ludwig Institute for Cancer Research. U.-M.K. is a postdoctoral fellow of the Academy of Finland and financially supported by the Finnish Foundation for Cardiovascular Research. A.H. is supported by NIH (DK44375).

Received February 21, 2001; revised May 1, 2001.

References

Ameen, N. (2000). Microvillus inclusion disease: a genetic defect affecting apical membrane protein traffic in intestinal epithelium. Traffic *1*, 76–83.

Apodaca, G., Katz, L.A., and Mostov, K.E. (1994). Receptor-mediated transcytosis of IgA in MDCK cells is via apical recycling endosomes. J. Cell Biol. *125*, 67–86.

Bartles, J.R., Feracci, H.M., Stieger, B., and Hubbard, A.L. (1987). Biogenesis of the rat hepatocyte plasma membrane in vivo: comparison of the pathways taken by apical and basolateral proteins using subcellular fractionation. J. Cell Biol. *105*, 1241–1251.

Beisiegel, U., Scheider, W.J., Goldstein, J.L., Anderson, R.G., and Brown, M.S. (1981). Monoclonal antibodies to the LDL receptor as probes for the study of receptor-mediated endocytosis and the genetics of familial hypercholesterolemia. J. Biol. Chem. *256*, 11923–11931.

Bonifacino, J.S., and Dell'Angelica, E.C. (1999). Molecular bases for the recognition of tyrosine-based sorting signals. J. Cell Biol. *145*, 923–926.

Charron, A.J., Nakamura, S., Bacallao, R., and Wandinger-Ness, A. (2000). Compromised cytoarchitecture and polarized trafficking in autosomal dominant polycystic kidney disease cells. J. Cell Biol. *149*, 111–124.

Davis, C.G., Lehrman, M.A., Russell, D.W., Anderson, R.G., Brown, M.S., and Goldstein, J.L. (1986). The JD mutation in familial hypercholesterolemia: Amino acid substitution in cytoplasmic domain impedes internalization of LDL receptors. Cell *45*, 15–24.

Davis, C.G., van Driel, I.R., Russell, D.W., Brown, M.S., and Goldstein, J.L. (1987). The low density lipoprotein receptor. Identification of amino acids in cytoplasmic domain required for rapid endocytosis. J. Biol. Chem. *262*, 4075–4082.

Diaz, E., and Pfeffer, S.R. (1998). TIP47: a cargo selection device for mannose 6-phosphate receptor trafficking. Cell *93*, 433–443.

Drubin, D.G., and Nelson, W.J. (1996). Origins of cell polarity. Cell *84*, 335–344.

Fölsch, H., Ohno, H., Bonifacino, J.S., and Mellman, I. (1999). A novel clathrin adaptor complex mediates basolateral targeting in polarized epithelial cells. Cell *99*, 189–198.

Fölsch, H., Pypaert, M., Schu, P., and Mellman, I. (2001). Distribution and function of AP-1 clathrin adaptor complexes in polarized epithelial cells. J. Cell Biol. *152*, 595–606.

He, T.C., Zhou, S., da Costa, L.T., Yu, J., Kinzler, K.W., and Vogelstein, B. (1998). A simplified system for generating recombinant adenoviruses. Proc. Natl. Acad. Sci. USA *95*, 2509–2514.

Herz, J., and Gerard, R.D. (1993). Adenovirus-mediated transfer of low density lipoprotein receptor gene acutely accelerates cholesterol clearance in normal mice. Proc. Natl. Acad. Sci. USA *90*, 2812–2816.

Hobbs, H.H., Brown, M.S., and Goldstein, J.L. (1992). Molecular genetics of the LDL receptor gene in familial hypercholesterolemia. Hum. Mutat. *1*, 445–466.

Huettinger, M., Schneider, W.J., Ho, Y.K., Goldstein, J.L., and Brown, M.S. (1984). Use of monoclonal anti-receptor antibodies to probe the expression of the low density lipoprotein receptor in tissues of normal and Watanabe heritable hyperlipidemic rabbits. J. Clin. Invest. *74*, 1017–1026.

Hunziker, W., Harter, C., Matter, K., and Mellman, I. (1991). Basolateral sorting in MDCK cells requires a distinct cytoplasmic domain determinant. Cell *66*, 907–920.

Ihrke, G., Neufeld, E.B., Meads, T., Shanks, M.R., Cassio, D., Laurent, M., Schroer, T.A., Pagano, R.E., and Hubbard, A.L. (1993). WIF-B cells: an in vitro model for studies of hepatocyte polarity. J. Cell Biol. *123*, 1761–1775.

Ihrke, G., Martin, G.V., Shanks, M.R., Schrader, M., Schroer, T.A., and Hubbard, A.L. (1998). Apical plasma membrane proteins and endolyn-78 travel through a subapical compartment in polarized WIF-B hepatocytes. J. Cell Biol. *141*, 115–133.

Ishibashi, S., Brown, M.S., Goldstein, J.L., Gerard, R.D., Hammer, R.E., and Herz, J. (1993). Hypercholesterolemia in low density lipoprotein receptor knockout mice and its reversal by adenovirus-mediated gene delivery. J. Clin. Invest. *92*, 883–893.

Keller, P., and Simons, K. (1997). Post-Golgi biosynthetic trafficking. J. Cell Sci. *110*, 3001–3009.

Kipp, H., and Arias, I.M. (2000). Newly synthesized canalicular ABC transporters are directly targeted from the Golgi to the hepatocyte apical domain in rat liver. J. Biol. Chem. *275*, 15917–15925.

Knight, A., Hughson, E., Hopkins, C.R., and Cutler, D.F. (1995). Membrane protein trafficking through the common apical endosome compartment of polarized Caco-2 cells. Mol. Biol. Cell *6*, 597–610.

Koivisto, U.-M., Viikari, J.S., and Kontula, K. (1995). Molecular characterization of minor gene rearrangements in Finnish patients with heterozygous familial hypercholesterolemia: identification of two common missense mutations (Gly823→Asp and Leu380→His) and eight rare mutations of the LDL receptor gene. Am. J. Hum. Genet. *57*, 789–797.

Kroschewski, R., Hall, A., and Mellman, I. (1999). Cdc42 controls secretory and endocytic transport to the basolateral plasma membrane of MDCK cells. Nat. Cell Biol. *1*, 8–13.

Marmorstein, A.D., Csaky, K.G., Baffi, J., Lam, L., Rahaal, F., and Rodriguez-Boulan, E. (2000). Saturation of, and competition for entry into, the apical secretory pathway. Proc. Natl. Acad. Sci. USA *97*, 3248–3253.

Matter, K., and Mellman, I. (1994). Mechanisms of cell polarity: sorting and transport in epithelial cells. Curr. Opin. Cell Biol. *6*, 545–554.

Matter, K., Hunziker, W., and Mellman, I. (1992). Basolateral sorting of LDL receptor in MDCK cells: the cytoplasmic domain contains two tyrosine-dependent targeting determinants. Cell *71*, 741–753.

Matter, K., Whitney, J.A., Yamamoto, E.M., and Mellman, I. (1993). Common signals control low density lipoprotein receptor sorting in endosomes and the Golgi complex of MDCK cells. Cell *74*, 1053–1064.

Matter, K., Yamamoto, E.M., and Mellman, I. (1994). Structural requirements and sequence motifs for polarized sorting and endocytosis of LDL and Fc receptors in MDCK cells. J. Cell Biol. *126*, 991–1004.

Mostov, K.E. (1994). Transepithelial transport of immunoglobulins. Annu. Rev. Immunol. *12*, 63–84.

Mostov, K., Apodaca, G., Aroeti, B., and Okamoto, C. (1992). Plasma membrane protein sorting in polarized epithelial cells. J. Cell Biol. *116*, 577–583.

Moyer, B.D., Denton, J., Karlson, K.H., Reynolds, D., Wang, S., Mickle, J.E., Milewski, M., Cutting, G.R., Guggino, W.B., Li, M., and Stanton, B.A. (1999). A PDZ-interacting domain in CFTR is an apical membrane polarization signal. J. Clin. Invest. *104*, 1353–1361.

Ohno, H., Tomemori, T., Nakatsu, F., Okazaki, Y., Aguilar, R.C., Fölsch, H., Mellman, I., Saito, T., Shirasawa, T., and Bonifacino, J.S. (1999). μ1B, a novel adaptor medium chain expressed in polarized epithelial cells. FEBS Lett. *449*, 215–220.

Powell-Braxton, L., Veniant, M., Latvala, R.D., Hirano, K.I., Won, W.B., Ross, J., Dybdal, N., Zlot, C.H., Young, S.G., and Davidson, N.O. (1998). A mouse model of human familial hypercholesterolemia: markedly elevated low density lipoprotein cholesterol levels and severe atherosclerosis on a low-fat chow diet. Nat. Med. *4*, 934–938.

Sheff, D.R., Daro, E.A., Hull, M., and Mellman, I. (1999). The receptor recycling pathway contains two distinct populations of early endosomes with different sorting functions. J. Cell Biol. *145*, 123–139.

Tuma, P.L., Finnegan, C.M., Yi, J.H., and Hubbard, A.L. (1999). Evidence for apical endocytosis in polarized hepatic cells: phosphoinositide 3-kinase inhibitors lead to the lysosomal accumulation of resident apical plasma membrane proteins. J. Cell Biol. *145*, 1089–1102.

van Driel, I.R., Goldstein, J.L., Südhof, T.C., and Brown, M.S. (1987). First cysteine-rich repeat in ligand-binding domain of LDL receptor binds Ca2+ and monoclonal antibodies, but not lipoproteins. J. Biol. Chem. *262*, 17443–17449.

Wan, L., Molloy, S.S., Thomas, L., Liu, G., Xiang, Y., Rybak, S.L., and Thomas, G. (1998). PACS-1 defines a novel gene family of cytosolic sorting proteins required for trans-Golgi network localization. Cell *94*, 205–216.

Yokode, M., Pathak, R.K., Hammer, R.E., Brown, M.S., Goldstein, J.L., and Anderson, R.G. (1992). Cytoplasmic sequence required for basolateral targeting of LDL receptor in livers of transgenic mice. J. Cell Biol. *117*, 39–46.

Yu, Q., Shao, R., Qian, H.S., George, S.E., and Rockey, D.C. (2000). Gene transfer of the neuronal NO synthase isoform to cirrhotic rat liver ameliorates portal hypertension. J. Clin. Invest. *105*, 741–748.